

# Reduction of Triadic Interactions Suppresses Intermittency and Anomalous Dissipation in Turbulence

Anikat Kankaria<sup>♣,1,\*</sup> Ritwik Mukherjee<sup>♣,1,†</sup> Sugan Durai  
Murugan,<sup>2,‡</sup> Marco Edoardo Rosti,<sup>3,§</sup> and Samriddhi Sankar Ray<sup>1,¶</sup>

<sup>1</sup>*International Centre for Theoretical Sciences, Tata Institute of Fundamental Research, Bangalore 560089, India*

<sup>2</sup>*Department of Mechanical Engineering, Johns Hopkins University, Baltimore, Maryland 21218, USA*

<sup>3</sup>*Complex Fluids and Flows Unit, Okinawa Institute of Science and Technology  
Graduate University, 1919-1 Tancha, Onna-son, Okinawa 904-0495, Japan*

(Dated:)

We investigate how the defining statistical features of three-dimensional turbulence respond to systematic reductions of the Fourier-space triadic interaction network. Using direct numerical simulations of both fractally and homogeneously decimated Navier–Stokes dynamics, we show that progressive thinning of the set of active modes leads to a systematic suppression of intermittency and, most strikingly, to the vanishing of the mean dissipation rate in the large-Reynolds-number limit. Structure-function exponents collapse onto their dimensional values, the multifractal singularity spectrum contracts, and the analyticity width extracted from the exponential spectral tail increases monotonically with decimation—each indicating a substantial regularization of the velocity field. Together, these results provide direct evidence that anomalous dissipation in incompressible turbulence is not a generic property of the Navier–Stokes equations, but instead requires the full combinatorial richness of their triadic nonlinear interactions.

A central challenge in three-dimensional (3D), fully-developed turbulence research is to identify what aspects of the Navier–Stokes nonlinearity are indispensable for the emergence of multiscaling, intermittency, and anomalous dissipation [1–4]. A possible candidate may well lie in the structure of the Fourier space triadic interactions between wavenumbers  $(\mathbf{k}, \mathbf{p}, \mathbf{q})$  which satisfy  $\mathbf{k} + \mathbf{p} + \mathbf{q} = 0$  and whose collective, nonlinear action determines much of what makes the problem of turbulence difficult [1]. It is tempting to ask if these key features of turbulence are robust properties of the three-dimensional (incompressible) Navier-Stokes equation, or whether the full combinatorial richness of the triadic interaction network is essential. More precisely, to what extent do intermittency, multifractality, and anomalous dissipation survive when the triadic network is progressively reduced? Related questions concerning the robustness of the dissipative anomaly itself have also been raised recently in direct numerical simulations of incompressible Navier–Stokes turbulence in periodic domains, where departures from the classical zeroth law of turbulence have been reported even in the absence of boundaries or explicit modifications of the equations [5].

A direct way to address this question is to surgically reduce the set of active interactions by projecting the dynamics onto a prescribed subset of Fourier modes, as introduced by Frisch *et al.* [6]. Fourier decimation provides a particularly clean, isotropic, and statistically homogeneous procedure: By retaining each Fourier mode with a given probability, one constructs a quenched projection that preserves incompressibility, the quadratic invariants,

and the algebraic form of the nonlinear term, while systematically reducing the number of triadic interactions in either a fractal or homogeneous fashion as we describe later. Probes of this type — including helicity-based surgeries [7, 8] and geometric triad restrictions [9, 10] — have already demonstrated that the cascade and intermittency can be strongly modified by selective changes to the nonlinear couplings [11–16].

Such a decimation procedure thins the triadic interaction network in controlled but complementary ways depending on the exact nature of mode removal: The fractal version reduces the number of active modes scale by scale according to an effective dimension  $D$  of the Fourier lattice [6], while the homogeneous version [11] removes modes uniformly across Fourier space. Neither procedure introduces any preferred physical direction or flow geometry, and both preserve incompressibility and the form of the nonlinear term. Taken together, they provide a systematic means of dismantling the interaction network, while keeping the underlying equations well defined, and hence address the question posed earlier.

In this paper we report results from direct numerical simulations (DNSs) of homogeneously and fractally decimated three-dimensional Navier-Stokes dynamics. We find that, as the density of active Fourier modes is reduced, the flow becomes progressively consistent with the non-intermittent, simple scaling theory of Kolmogorov [1] accompanied by an *almost* vanishing dissipation — in contrast to anomalous dissipation in fully-developed turbulence [2, 4] — with increasing Reynolds number.

We begin with the incompressible, unit density 3D Navier-Stokes equation for the velocity field  $\mathbf{u}$ , with its Fourier representation  $\hat{\mathbf{u}}(\mathbf{k}, \mathbf{t})$ , from which we define the

♣ These authors contributed equally to this work

decimated field

$$\mathbf{v}(\mathbf{x}, t) = \mathcal{P} \mathbf{u}(\mathbf{x}, t) = \sum_{\mathbf{k}} e^{i\mathbf{k}\cdot\mathbf{x}} \gamma_{\mathbf{k}} \hat{\mathbf{u}}(\mathbf{k}, t), \quad (1)$$

through the generalised Galerkin projector  $\mathcal{P}$ . The quenched-in-time factors  $\gamma_{\mathbf{k}}$  follow

$$\gamma_{\mathbf{k}} = \begin{cases} 1, & \text{with probability } h_k \\ 0, & \text{with probability } 1 - h_k \end{cases} \quad \text{with } k \equiv |\mathbf{k}|, \quad (2)$$

and preserve Hermitian symmetry to ensure that  $\mathcal{P}$  is a self-adjoint operator which commutes with the nonlinear and viscous terms. Such a micro surgery ensures that the invariants of the original 3D problem — namely energy and helicity — are preserved [6, 12].

This allows a simple reformulation of the Navier-Stokes equation, with kinematic viscosity  $\nu$  and pressure  $p$ , for the Fourier decimated velocity field

$$\frac{\partial \mathbf{v}}{\partial t} = \mathcal{P}[-\nabla p - (\mathbf{v} \cdot \nabla \mathbf{v})] + \nu \nabla^2 \mathbf{v} + \mathbf{F}, \quad (3)$$

with initial conditions  $\mathbf{v}_0 = \mathcal{P} \mathbf{u}_0$ . The projection of the nonlinear term ensures that the evolution of the velocity field is restricted on the subset of Fourier modes defined via Eqs. (1)-(2). Similarly, the external force  $\mathbf{F}$  which drives the flow to a statistically steady state has the same compact support on the decimated Fourier lattice.

There is freedom in the way we choose the factor  $h_k$ . In its original formulation — the so-called *fractal Fourier* decimation approach of Frisch *et al.* [6] — an effective dimensionality  $D$  is obtained by choosing  $h_k \propto (k/k_0)^{D-3}$ , with  $0 < D \leq 3$ ; the arbitrary wavenumber  $k_0$  can be set to unity. This restriction of the dynamics on a  $D$ -dimensional Fourier sub-space results in an effective velocity field  $\mathbf{v}$  with embedding dimension 3, but with degrees of freedom  $\sim k^D$ . A second option — *homogeneous* decimation — is to decimate with  $h_k = \rho$ ,  $\forall k$  with  $0 < \rho \leq 1$  [11–16]. Trivially, setting  $D = 3$  or  $\rho = 1$  leads to the usual three-dimensional Navier-Stokes equation.

We solve the decimated Navier-Stokes equation on a  $2\pi$  triply-periodic cubic box, with  $512^3$  and  $1024^3$  collocation points as well as different numerical solvers for consistency check. Further, we drive the system to a statistically steady state using two different large-scale energy injections limited to the first two modes [17], one that ensures a constant energy input and one that does not [18]. This allows us to achieve Taylor-scale Reynolds numbers  $50 \leq \text{Re}_\lambda \leq 550$ , with  $\text{Re}_\lambda = v_{\text{rms}} \lambda / \nu$ ; the mean kinetic energy dissipation rate  $\langle \varepsilon \rangle = 2\nu \langle S_{ij} S_{ij} \rangle$ , where  $S_{ij} = \frac{1}{2}(\partial_i v_j + \partial_j v_i)$  is the strain-rate tensor, and the root-mean-square velocity  $v_{\text{rms}}$  allows us to define the Taylor micro-scale  $\lambda^2 = v_{\text{rms}}^2 / \langle (\frac{\partial v}{\partial x})^2 \rangle$ . Finally, we use several different values of the fractal dimension  $2.8 \leq D \leq 3.0$  and, for the homogeneous decimation,  $0.4 \leq \rho \leq 1$ ; the simulations with  $D = 3$  or  $\rho = 1$  are solutions for the un-decimated Navier-Stokes equation,

which serves as a reference state for many of the discussions that follow.

A useful insight on the role of triads comes from, for example, two-dimensional slices of the energy dissipation rate  $\varepsilon$  [16]. This is illustrated, in Figs. 1(a) and (b), by comparing pseudocolor plots, on a logscale, of  $\varepsilon$  from a fully three-dimensional simulation ( $\rho = 1$ ) to a highly decimated flow ( $\rho = 0.5$ ), respectively. A comparison of these two figures show that decimation leads to a suppression of the typical worm-like filaments, characteristic of intermittent and fully-developed turbulence, and renders a more featureless field devoid of structure [16]. This absence of intermittency suggests that the non-Gaussian tails of the strain field  $S_{ij}$  in turbulence should converge to a Gaussian with decimation. In the inset of Fig. 1(c) we show a representative plot of the probability distribution function of  $S_{xy}$ , with varying degrees of decimation, including the  $D = 3$  case, which confirms the intuition brought out by Fig. 1(b). A further implication of such a trend is the transition from a nominally log-normal distribution of the dissipation field for  $D = 3$  [1] to one which is Chi-squared of 5th order and hence exponentially distributed. We find compelling evidence of this in our simulations as shown in Fig. 1(c); this transition to an exponential distribution was already noted by Picardo *et al.* [16].

Such a systematic suppression of intermittency naturally raises the question of how the dissipative anomaly behaves under decimation, since the persistence of finite mean dissipation as  $\nu \rightarrow 0$  is, assumed to be, intimately tied to the presence of strong gradients and intermittent fluctuations in the undiluted three-dimensional flow. This motivates a direct examination of the mean dissipation as a function of Reynolds number under controlled decimation, as we now demonstrate.

In Fig. 2 we show a plot of the normalised mean kinetic energy dissipation  $\langle \varepsilon \rangle L / v_{\text{rms}}^3$ , where the integral scale  $L = \frac{\pi}{2v_{\text{rms}}^2} \int_0^\infty \frac{E(k)}{k} dk$ , versus the Taylor-scale Reynolds number  $\text{Re}_\lambda$  for different levels of decimation. The data for three-dimensional turbulence saturates to a finite, non-zero value as  $\text{Re}_\lambda \rightarrow \infty$  indicating dissipative anomaly and consistent with a fitting function, as discussed in Refs. [19, 20], which is indicated by a black dashed line. With increasing decimation, however, a clear trend emerges. Once the triadic network is sufficiently tampered for  $\rho \lesssim 0.5$  the mean dissipation decreases systematically with  $\text{Re}_\lambda$  and shows no sign of approaching a non-zero asymptote as marked by the black-dashed line. Instead, the data indicate that it is likely that  $\langle \varepsilon \rangle L / v_{\text{rms}}^3 \rightarrow 0$  as  $\text{Re}_\lambda \rightarrow \infty$  for such a level of decimation is in clear violation of dissipative anomaly.

Further insight into the mechanism underlying Fig. 2 is provided by the inset, which shows the probability density function of the vorticity–strain interaction (often referred to as vorticity production); precise definitions of

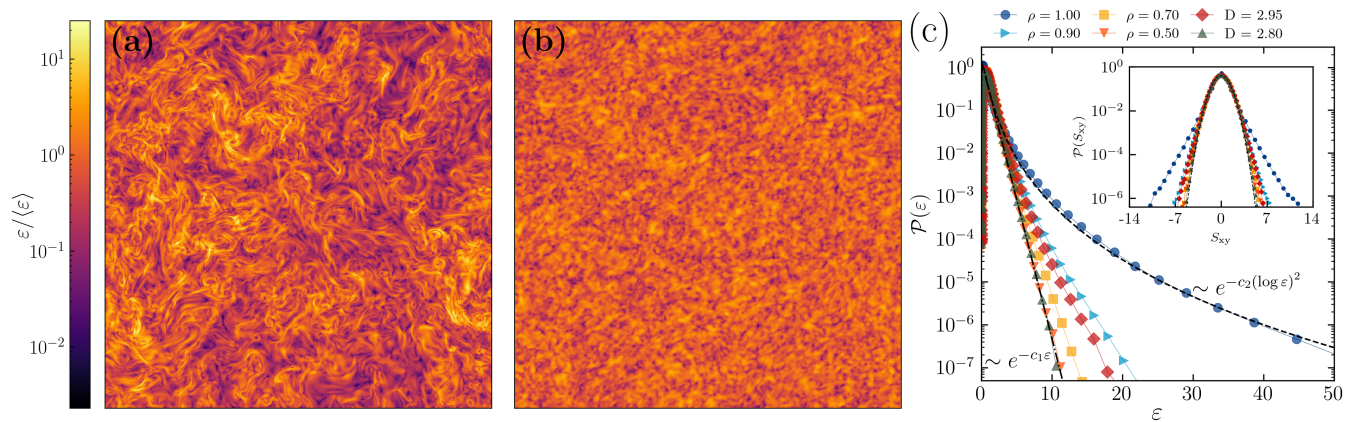


FIG. 1. Pseudo-color plots of the energy dissipation field  $\varepsilon$  on a two-dimensional slice for (a) the undecimated case  $\rho = 1$  and (b) a homogeneously decimated flow with  $\rho = 0.5$ , shown on a logarithmic color scale. Decimation suppresses the intense filamentary structures characteristic of intermittent three-dimensional turbulence, resulting in a smoother dissipation field. (c) Probability density functions of  $\langle \varepsilon \rangle$  for increasing decimation, showing a transition from log-normal to exponential tails. (Inset) PDFs of the longitudinal strain-rate component  $S_{xy}$  approaching a Gaussian form with increasing decimation.

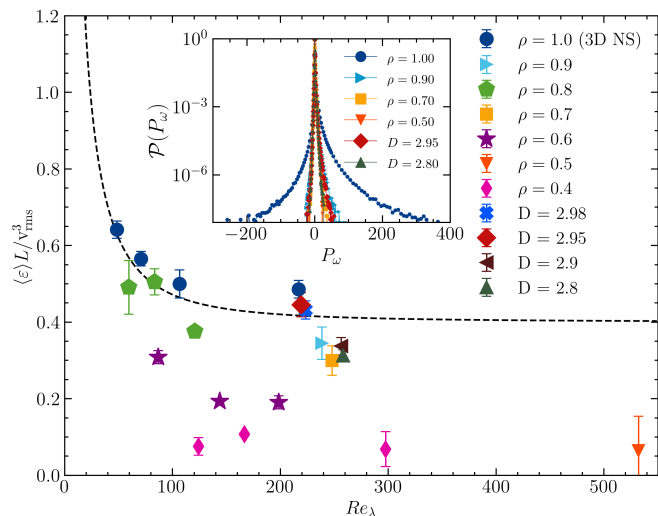


FIG. 2. Mean dissipation rate  $\varepsilon$  versus the Taylor-scale Reynolds number  $Re_\lambda$  for different levels of Fourier decimation, compared with the undecimated three-dimensional Navier–Stokes case. With increasing decimation,  $\varepsilon$  decreases systematically with  $Re_\lambda$ , indicating a breakdown of dissipative anomaly. The black dashed line represent the parameterized dissipative anomaly curve [19, 20]. (Inset) Probability density functions of the vorticity–strain interaction (vorticity production) for selected decimation levels, illustrating the suppression of extreme vortex-stretching events.

the quantities involved, together with their geometric interpretation as well as the associated  $QR$  plots, are given in Appendix A. This interaction governs vortex stretching in three-dimensional incompressible flows and is a key ingredient of the forward transfer of kinetic energy to small scales. In the undecimated Navier–Stokes dynamics, the distribution displays pronounced non-Gaussian tails, reflecting the presence of rare but intense stretching

events that generate strong velocity gradients and sustain finite dissipation at high Reynolds numbers. As the Fourier-space interaction network is progressively decimated, these tails are systematically suppressed and the distribution becomes increasingly concentrated. This trend indicates a weakening of vortex stretching and, concomitantly, a reduced efficiency of the nonlinear cascade in producing extreme small-scale activity. The inset thus provides a dynamical counterpart to the behaviour seen in the main panel: the decay of the mean dissipation rate with Reynolds number is accompanied by the depletion of the very events responsible for feeding the cascade, driving the flow toward a more regular regime in which anomalous dissipation is no longer supported.

To the best of our knowledge, this is the first direct demonstration of a violation of the dissipative anomaly in an incompressible Navier–Stokes system. While our results do not address the origin of the anomaly in the fully three-dimensional case, they provide compelling evidence that its existence requires the full triadic structure of the Navier–Stokes nonlinearity. In particular, the suppression of  $\varepsilon$  under decimation shows that removing even a statistically homogeneous subset of triads fundamentally alters the mechanism responsible for sustaining finite dissipation in the vanishing-viscosity limit. Our results clearly demonstrate that the fine-scale structure of turbulence is highly sensitive to the connectivity of the triadic interaction network, even though the large-scale cascade and a power-law energy spectrum remain comparatively robust. Viewed more broadly, these findings resonate with recent numerical evidence questioning the universality of the zeroth law of turbulence in incompressible Navier–Stokes flows [5]. In this context, our work identifies the combinatorial completeness of the triadic interaction network as a key structural ingredi-

ent required for sustaining anomalous dissipation in the infinite-Reynolds-number limit.

These observations connect naturally to rigorous constraints relating anomalous dissipation to the behaviour of velocity increments. Onsager's criterion [21] and its mathematical refinements by Eyink [22] and by Constantin, E, and Titi [23] place a critical Hölder threshold  $h = 1/3$  for the possible existence of anomalous dissipation in the inviscid limit, while the Duchon–Robert local energy balance [24] expresses anomalous dissipation as a distributional limit of symmetric velocity increments and ties it explicitly to third-order statistics. Taken together, these results imply that nonzero dissipation, in the infinite Reynolds number limit, requires sufficiently singular velocity increments and nontrivial third-order scaling, and they place restrictions on how rapidly the hierarchy of structure functions may grow [25].

Therefore, a further implication of this framework concerns the high-order exponents themselves. Since anomalous dissipation demands a degree of singularity incompatible with excessively smooth behaviour, the effective scaling ratios  $\zeta_p/p$  — where  $\zeta_p$  is the scaling exponent of the  $p$ -th order equal-time structure function defined via  $S_p(r) \equiv \langle |\delta_r v|^p \rangle$ , with  $\delta_r v$  the longitudinal velocity increment between two points separated by an inertial range distance  $r$  — for sufficiently large  $p$  must lie strictly below the critical value  $1/3$  associated with energy conservation. Recent formulations of the local energy balance make this explicit [4]: If  $\langle \varepsilon \rangle$  is nonzero, then for suitable  $p > 3$  one necessarily has  $\zeta_p/p < 1/3$ , provided the dissipation has even mild spatial concentration. Thus, as Fourier decimation drives the flow toward smoother behaviour and suppresses intermittency, one expects the ratios  $\zeta_p/p$  to drift upward toward the dimensional value  $1/3$ , signalling the progressive loss—and eventual disappearance—of anomalous dissipation. This connection provides a natural motivation for a direct examination of the equal-time structure-function exponents under decimation, to which we now turn.

Figure 3 shows the dependence of  $\zeta_p/p$  on  $p$ , obtained via extended self-similarity [26, 27], for different values of  $\rho$  and  $D$ , including, for reference the  $\rho = 1$  (or  $D = 3$ ) three-dimensional problem. For the undecimated  $D = 3$  case, the exponents display the familiar intermittency-induced departure from the dimensional line  $1/3$ . As the decimation increases, however, the nonlinear curvature of the  $\zeta_p/p$  spectrum systematically diminishes: The high-order exponents move upward toward their dimensional values, and the entire curve collapses progressively onto the straight line  $\zeta_p/p = 1/3$ . This behaviour is fully consistent with the regularity-based expectations discussed above and mirrors the concurrent suppression of the dissipative anomaly. Furthermore a direct measurement of the hyperflatness  $\frac{\langle (\delta_r v)^6 \rangle}{\langle (\delta_r v)^2 \rangle^3}$  of the probability density functions of the velocity increments show, as seen in the inset

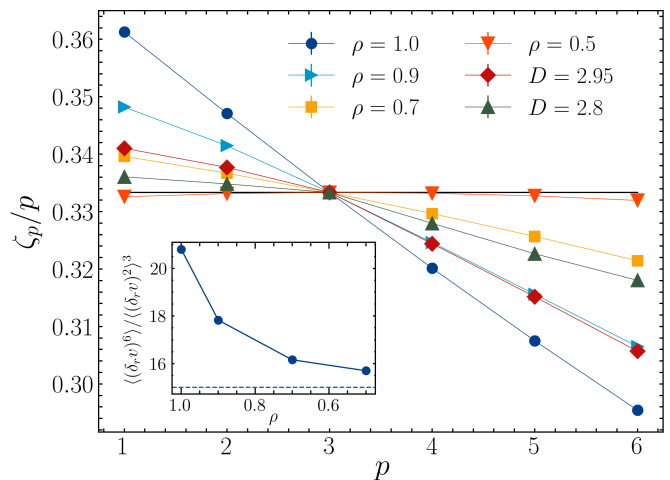


FIG. 3. Ratios  $\zeta_p/p$  of longitudinal equal-time structure-function exponents as a function of order  $p$  for different levels of homogeneous and fractal Fourier decimation (see legend). The undecimated case exhibits clear departures from the dimensional prediction  $\zeta_p/p = 1/3$ , while increasing decimation leads to a progressive collapse toward the dimensional value. (Inset) Hyperflatness of the PDFs of longitudinal velocity increments at inertial-range separations, approaching the Gaussian value 15 with increasing decimation.

of Fig. 3, a convergence to the Gaussian value 15 with increasing decimation.

The multifractal framework [1, 28] provides a natural bridge between the suppression of intermittency under decimation and the behaviour of the dissipation field. Since the dissipation is dominated by rare, intense gradient events, any systematic smoothing of the flow—such as that produced by reducing the connectivity of the triadic interaction network—must necessarily diminish the range of local scaling exponents present in the velocity field. These are commonly characterized in terms of the dissipation exponent  $\alpha$ , related to the velocity Hölder exponent  $h$  by  $\alpha = 3h$ , and their distribution is encoded in the singularity spectrum  $f(\alpha)$  [29–31]. This immediately implies that the singularity spectrum should contract as decimation increases: Fewer extreme events correspond to a narrower spread of  $\alpha$  values. This logical expectation is borne out clearly in the data. As shown in Fig. 4, the singularity spectra obtained from a multifractal analysis of the dissipation field progressively narrow with increasing decimation, demonstrating a collapse of multifractality and confirming the direct link between the loss of intermittency and the attenuation of anomalous dissipation.

The progressive narrowing of the singularity spectrum under decimation indicates a clear loss of fine-scale variability in the velocity field, suggesting that the flow becomes increasingly regular as the triadic interaction network is thinned. While the multifractal framework captures this through the contraction of  $f(\alpha)$ , it is equally

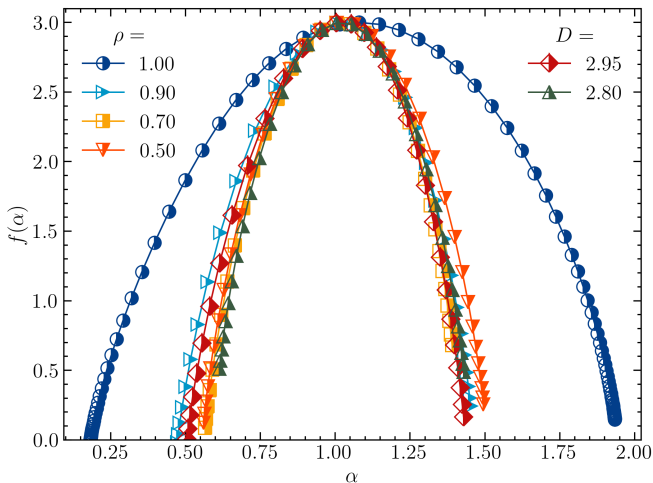


FIG. 4. Singularity spectra  $f(\alpha)$  obtained from a multifractal analysis of the dissipation field for different levels of decimation. The undecimated case exhibits a broad spectrum, whereas increasing decimation leads to a systematic narrowing, indicating a progressive loss of multifractality.

valuable to complement this local, increment-based picture with a global diagnostic of smoothness. A natural candidate is provided by the analyticity-strip method, which quantifies the distance  $\delta$  of the closest complex singularity to the real axis through the exponential decay of the Fourier spectrum [1, 32, 33]. Because  $\delta$  offers an independent, Fourier-space measure of regularity, examining its systematic variation with decimation provides a crucial cross-check of the multifractal results and further clarifies how the small-scale analytic structure of the flow is altered as the nonlinear couplings are reduced.

To this end, we estimate the analyticity width  $\delta$  for each decimation level by analysing statistically steady, shell-averaged energy spectra. In the high-wavenumber range where the spectrum exhibits exponential decay, the analyticity-strip framework predicts  $\ln E(k) \approx -2\delta k + m \ln k + C$  so that  $\delta$  may be extracted directly from the slope of  $\ln E(k)$  versus  $k$  [32]. For every decimated state, we compute the isotropic spectrum  $E(k)$  over an ensemble of steady-state snapshots, identify the exponential tail through the plateau of the local slope  $-\partial_k \ln E(k)$ , and perform a weighted least-squares fit over this interval to obtain  $\delta$ , with uncertainties estimated by bootstrap resampling. The resulting dependence of  $\delta$  on the decimation parameter, shown in Fig. 5, reveals a clear and monotonic increase of the analyticity width as the fraction of active Fourier modes is reduced. This trend parallels the concomitant narrowing of the singularity spectrum and therefore provides strong, independent evidence for the progressive smoothing of the flow and the suppression of intermittency under decimation. The inset of Fig. 5 shows a concomitant increase of the Kolmogorov constant  $C_{\text{Kol}}$ , obtained from fits of the energy spectrum

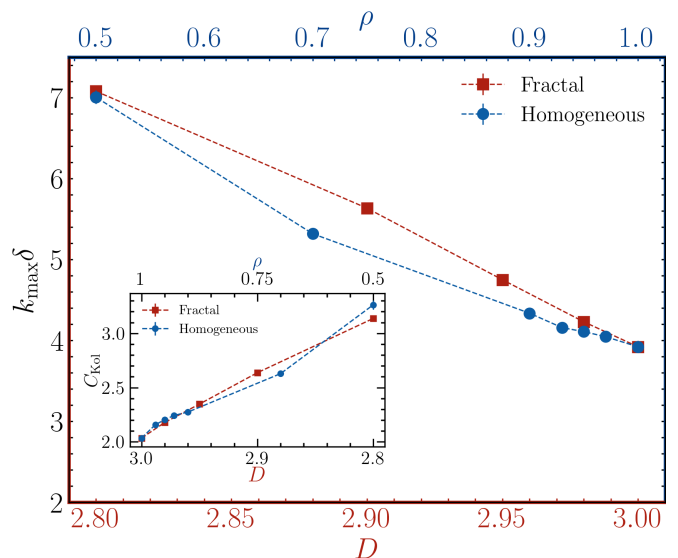


FIG. 5. Analyticity width  $\delta$  as a function of the decimation parameter (either  $D$  or  $\rho$ , see legend), extracted from the exponential decay of the statistically steady energy spectra. The monotonic increase of  $\delta$  with decimation indicates a widening of the analyticity strip and a progressively smoother flow. (Inset) Kolmogorov constant as a function of decimation.

$E(k) = C_{\text{Kol}} \varepsilon^{2/3} k^{-5/3}$ , with decimation indicating that the reduced flux is accommodated by a renormalization of the inertial-range spectrum rather than a breakdown of Kolmogorov scaling [6].

In summary, our results demonstrate that the central signatures of fully developed three-dimensional turbulence — anomalous dissipation, multiscaling of structure functions, and multifractality — are not robust to a systematic reduction of the Fourier-space triadic interaction network. Both fractal and homogeneous decimation lead to a progressive weakening of intermittency, manifested in the collapse of the structure-function exponents toward their dimensional values, the marked narrowing of the multifractal singularity spectrum, and, most notably, the eventual disappearance of the dissipative anomaly. These observations provide direct, quantitative evidence that the persistence of finite dissipation in the vanishing-viscosity limit, along with attributes of fully developed turbulence depends, sensitively on the full combinatorial richness of the Navier–Stokes nonlinearity.

M.E.R. was supported by the Okinawa Institute of Science and Technology Graduate University (OIST) with subsidy funding from the Cabinet Office, Government of Japan. M.E.R. also acknowledges funding from the Japan Society for the Promotion of Science (JSPS), grant 24K17210 and 24K00810, and the computer time provided by the Scientific Computing & Data Analysis section of the Core Facilities at OIST, and by HPCI, under the Research Project grants hp250021 and hp250035. SSR acknowledges the CEFIPRA Project No 6704-1 for

support and the hospitality of the Okinawa Institute of Science and Technology (OIST) where parts of this work were carried out. The simulations were performed on the ICTS clusters Mario, Tetris, and Contra. AK, RM and SSR acknowledge the support of the Department of Atomic Energy, Government of India, under project no.RTI4019 and RTI4013.

---

\* anikat.kankaria@gmail.com  
 † ritwik.mukherjee@icts.res.in  
 ‡ vsdmfriend@gmail.com  
 § marco.rosti@oist.jp  
 ¶ samriddhisankarray@gmail.com

- [1] U. Frisch, *Turbulence: The Legacy of A. N. Kolmogorov* (Cambridge University Press, 1996).
- [2] T. Ishihara, T. Gotoh, and Y. Kaneda, *Annual Review of Fluid Mechanics* **41**, 165 (2009).
- [3] R. Pandit, P. Perlekar, and S. S. Ray, *Pramana* **73**, 157 (2009).
- [4] G. Eyink, *Journal of Fluid Mechanics* **988**, P1 (2024).
- [5] K. P. Iyer, T. D. Drivas, G. L. Eyink, and K. R. Sreenivasan, *Phys. Rev. Lett.* **135**, 134001 (2025).
- [6] U. Frisch, A. Pomyalov, I. Procaccia, and S. S. Ray, *Phys. Rev. Lett.* **108**, 074501 (2012).
- [7] L. Biferale, S. Musacchio, and F. Toschi, *Phys. Rev. Lett.* **108**, 164501 (2012).
- [8] L. Biferale and E. S. Titi, *Journal of Statistical Physics* **151**, 1089 (2013).
- [9] S. Grossmann, D. Lohse, and A. Reeh, *Phys. Rev. Lett.* **77**, 5369 (1996).
- [10] O. D. Gürçan, *Phys. Rev. E* **95**, 063102 (2017).
- [11] A. S. Lanotte, R. Benzi, S. K. Malapaka, F. Toschi, and L. Biferale, *Phys. Rev. Lett.* **115**, 264502 (2015).
- [12] S. S. Ray, *Pramana* **84**, 395 (2015).
- [13] M. Buzzicotti, L. Biferale, U. Frisch, and S. S. Ray, *Phys. Rev. E* **93**, 033109 (2016).
- [14] M. Buzzicotti, A. Bhatnagar, L. Biferale, A. S. Lanotte, and S. S. Ray, *New Journal of Physics* **18**, 113047 (2016).
- [15] S. S. Ray, *Phys. Rev. Fluids* **3**, 072601 (2018).
- [16] J. R. Picardo, A. Bhatnagar, and S. S. Ray, *Phys. Rev. Fluids* **5**, 042601 (2020).
- [17] A. G. Lamorgese, D. A. Caughey, and S. B. Pope, *Physics of Fluids* **17**, 015106 (2004).
- [18] V. Eswaran and S. Pope, *Computers & Fluids* **16**, 257 (1988).
- [19] D. A. Donzis, K. R. Sreenivasan, and P. K. Yeung, *Journal of Fluid Mechanics* **532**, 199–216 (2005).
- [20] I. Cannon, S. Olivieri, and M. E. Rosti, *Phys. Rev. Fluids* **9**, 064301 (2024).
- [21] G. L. Eyink and K. R. Sreenivasan, *Rev. Mod. Phys.* **78**, 87 (2006).
- [22] G. L. Eyink, *Physica D: Nonlinear Phenomena* **78**, 222 (1994).
- [23] P. Constantin, E. Weinan, and E. S. Titi, *Communications in Mathematical Physics* **165**, 207 (1994).
- [24] J. Duchon and R. Robert, *Nonlinearity* **13**, 249 (2000).
- [25] G. Eyink, *Journal of Fluid Mechanics* **988**, P1 (2024).
- [26] R. Benzi, S. Ciliberto, R. Tripiccone, C. Baudet, F. Masaioli, and S. Succi, *Phys. Rev. E* **48**, R29 (1993).
- [27] S. Chakraborty, U. Frisch, and S. S. Ray, *Journal of Fluid Mechanics* **649**, 275–285 (2010).
- [28] U. Frisch and G. Parisi, *Proceedings of the International School of Physics Enrico Fermi, Course LXXXVIII, Varenna, 1985* (1985).
- [29] K. Sreenivasan, *Annual review of fluid mechanics* **23**, 539 (1991).
- [30] C. Meneveau and K. Sreenivasan, *Nuclear Physics B - Proceedings Supplements* **2**, 49 (1987).
- [31] S. Mukherjee, S. D. Murugan, R. Mukherjee, and S. S. Ray, *Phys. Rev. Lett.* **132**, 184002 (2024).
- [32] C. Sulem, P. L. Sulem, and H. Frisch, *Journal of Computational Physics* **50**, 138 (1983).
- [33] S. D. Murugan, U. Frisch, S. Nazarenko, N. Besse, and S. S. Ray, *Phys. Rev. Res.* **2**, 033202 (2020).

## APPENDIX A: QR DIAGNOSIS

A central quantity for characterizing small-scale dynamics in three-dimensional incompressible turbulence is the vorticity–strain interaction, commonly referred to as vorticity production. Let

$$\boldsymbol{\omega} = \nabla \times \boldsymbol{v} \quad (4)$$

denote the vorticity field and

$$S_{ij} = \frac{1}{2} (\partial_i v_j + \partial_j v_i) \quad (5)$$

the strain-rate tensor. The local rate of vorticity production is then given by

$$P_\omega = \omega_i S_{ij} \omega_j, \quad (6)$$

which measures the stretching or compression of vorticity by the strain field. Positive values of  $P_\omega$  correspond to vortex stretching, a uniquely three-dimensional mechanism responsible for the amplification of velocity gradients and the forward cascade of kinetic energy to small scales. In fully developed turbulence, the statistics of  $P_\omega$  are strongly non-Gaussian, reflecting the presence of rare but intense stretching events that play a crucial role in sustaining intermittency and anomalous dissipation.

In the inset of Fig. 2 of the main text, we show the probability density functions of  $P_\omega$  for representative degrees of Fourier decimation. In the undecimated Navier–Stokes dynamics, the distribution exhibits pronounced non-Gaussian tails, reflecting the presence of rare but intense vortex-stretching events that are responsible for generating extreme velocity gradients. As the interaction network is progressively decimated, these tails are systematically suppressed and the distribution becomes increasingly concentrated around its mean. This clear depletion of extreme vorticity-production events provides direct evidence that decimation weakens the nonlinear mechanisms responsible for populating the smallest scales of the flow.

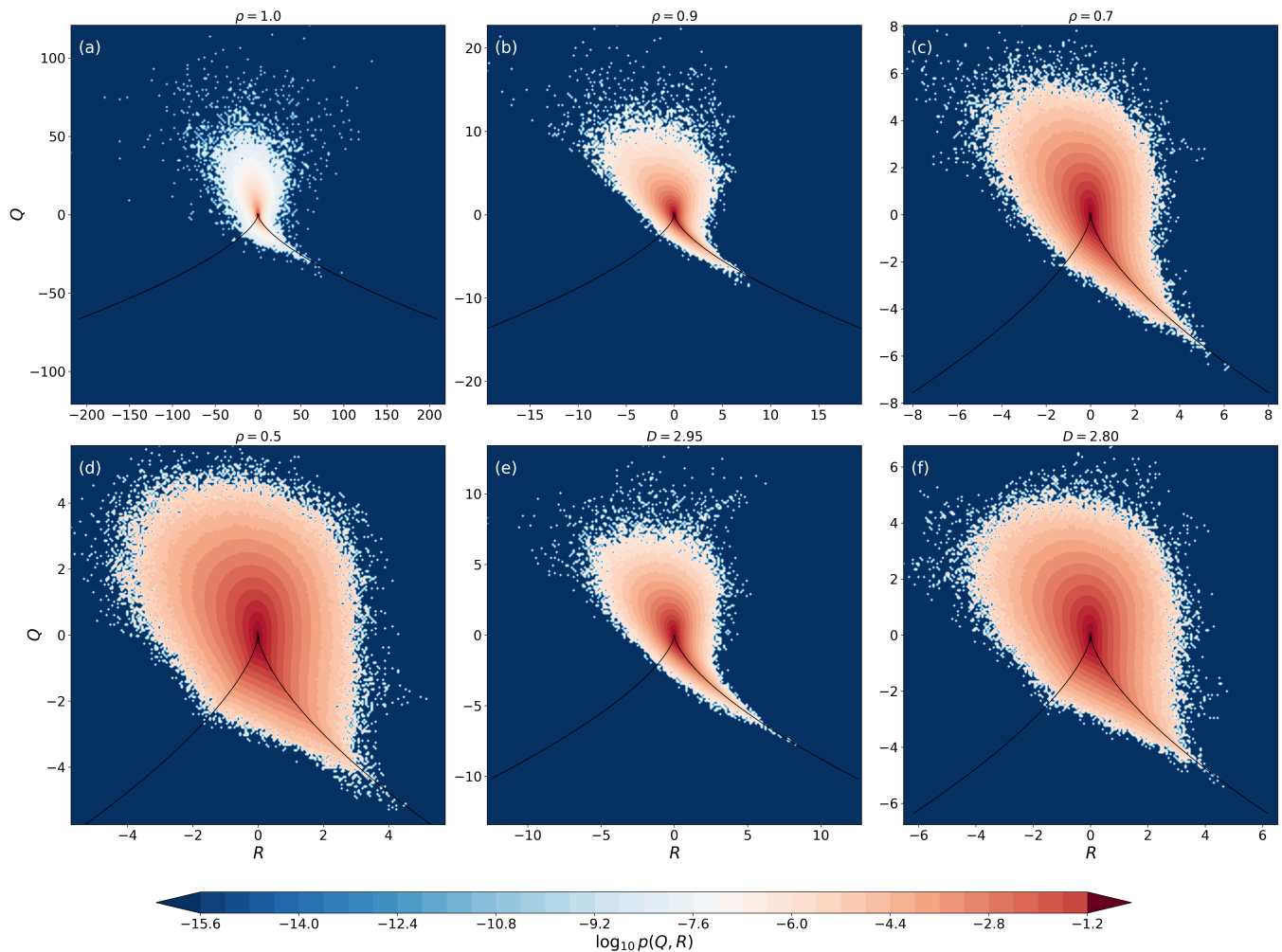


FIG. 6. Joint probability density functions of the second and third invariants ( $Q, R$ ) of the velocity-gradient tensor for different degrees of Fourier decimation (see labels). The undecimated Navier–Stokes case exhibits the characteristic teardrop-shaped distribution with broad support, reflecting intense small-scale velocity gradients and strong vortex stretching. As the level of decimation is increased, the support of the distribution contracts systematically and the accessible range of  $Q$  and  $R$  decreases, indicating a progressive suppression of extreme gradient events. This contraction of the  $QR$  distributions provides clear geometric evidence that thinning the triadic interaction network kills small scales and drives the flow toward a smoother, more regular regime.

To gain further geometric insight into the local flow topology underlying vorticity production, it is useful to analyze the velocity-gradient tensor  $A_{ij} = \partial_j v_i$  through its second and third invariants, defined as

$$Q = -\frac{1}{2}\text{Tr}(A^2), \quad R = -\frac{1}{3}\text{Tr}(A^3). \quad (7)$$

The joint probability distribution of  $Q$  and  $R$ , commonly visualized in the form of  $QR$  plots, provides a compact representation of local flow structures. In incompressible turbulence, the  $(Q, R)$ -plane is partitioned by the discriminant curve

$$\Delta = \frac{27}{4}R^2 + Q^3 = 0, \quad (8)$$

which separates regions dominated by rotational motion from those dominated by strain. The characteristic teardrop-shaped distribution observed in the undecimated Navier–Stokes dynamics is a robust statistical signature of intense small-scale activity and strong vortex stretching.

Figure 6 shows the  $QR$  plots for various degrees of homogeneous and fractal Fourier decimation. In the undecimated case, the joint distribution extends over a wide range of  $Q$  and  $R$ , reflecting the presence of strong velocity gradients and highly intermittent small-scale structures. As the level of decimation is increased, however, the support of the distribution contracts systematically. This contraction is accompanied by a marked reduction in the range of accessible  $Q$  and  $R$  values, clearly visible

through the progressive narrowing of the axes in Fig. 6.

This reduction in the extent of the  $QR$  distributions provides direct evidence that Fourier decimation suppresses the most intense small-scale events. By thinning the triadic interaction network, decimation weakens vortex stretching, limits the generation of extreme velocity gradients, and effectively removes the tails of

the velocity-gradient statistics. The shrinking of the  $QR$  support thus offers a geometric and statistical manifestation of the same regularization observed in the dissipation field, vorticity-production statistics, and structure-function scaling: decimation systematically kills small scales, driving the flow toward a smoother, more regular regime in which intermittency and anomalous dissipation can no longer be sustained.